



Pediatric low-grade gliomas can be molecularly stratified for risk

Rui Ryan Yang^{1,2,3} · Abudumijiti Aibaidula³ · Wei-wei Wang⁴ · Aden Ka-Yin Chan¹ · Zhi-feng Shi³ · Zhen-yu Zhang⁵ · Danny Tat Ming Chan⁶ · Wai Sang Poon⁶ · Xian-zhi Liu⁵ · Wen-cai Li⁴ · Rui-qi Zhang¹ · Yan-Xi Li¹ · Nellie Yuk-Fei Chung^{1,2} · Hong Chen⁷ · Jingsong Wu³ · Liangfu Zhou³ · Kay Ka-Wai Li^{1,2} · Ho-Keung Ng^{1,2}

Received: 21 December 2017 / Accepted: 5 June 2018 / Published online: 14 June 2018
© Springer-Verlag GmbH Germany, part of Springer Nature 2018

Abstract

Pediatric low-grade gliomas (PLGGs) consist of a number of entities with overlapping histological features. PLGGs have much better prognosis than the adult counterparts, but a significant proportion of PLGGs suffers from tumor progression and recurrence. It has been shown that pediatric and adult low-grade gliomas are molecularly distinct. Yet the clinical significance of some of newer biomarkers discovered by genomic studies has not been fully investigated. In this study, we evaluated in a large cohort of 289 PLGGs a list of biomarkers and examined their clinical relevance. TERT promoter (TERTp), H3F3A and BRAF V600E mutations were detected by direct sequencing. ATRX nuclear loss was examined by immunohistochemistry. CDKN2A deletion, KIAA1549-BRAF fusion, and MYB amplification were determined by fluorescence in situ hybridization (FISH). TERTp, H3F3A, and BRAF V600E mutations were identified in 2.5, 6.4, and 7.4% of PLGGs, respectively. ATRX loss was found in 4.9% of PLGGs. CDKN2A deletion, KIAA1549-BRAF fusion and MYB amplification were detected in 8.8, 32.0 and 10.6% of PLGGs, respectively. Survival analysis revealed that TERTp mutation, H3F3A mutation, and ATRX loss were significantly associated with poor PFS ($p < 0.0001$, $p < 0.0001$, and $p = 0.0002$) and OS ($p < 0.0001$, $p < 0.0001$, and $p < 0.0001$). BRAF V600E was associated with shorter PFS ($p = 0.011$) and OS ($p = 0.032$) in a subset of PLGGs. KIAA1549-BRAF fusion was a good prognostic marker for longer PFS ($p = 0.0017$) and OS ($p = 0.0029$). MYB amplification was also a favorable marker for a longer PFS ($p = 0.040$). Importantly, we showed that these molecular biomarkers can be used to stratify PLGGs into low- (KIAA1549-BRAF fusion or MYB amplification), intermediate-I (BRAF V600E and/or CDKN2A deletion), intermediate-II (no biomarker), and high-risk (TERTp or H3F3A mutation or ATRX loss) groups with distinct PFS ($p < 0.0001$) and OS ($p < 0.0001$). This scheme should aid in clinical decision-making.

Keywords Pediatric low-grade gliomas · H3F3A · ATRX · BRAF · CDKN2A · Molecular risk stratification

Introduction

Pediatric low-grade gliomas (PLGGs) are a heterogeneous group [34], and while the WHO 2016 classification did not specify a classification specific for PLGGs, the following

histological groups which can occur in the young age group are included in WHO 2016: pilocytic astrocytoma (Grade I), diffuse astrocytoma (Grade II), oligodendroglioma (Grade II), oligoastrocytoma (Grade II), pleomorphic xanthoastrocytoma (Grade II), dysembryoplastic neuroepithelial tumor (Grade I), neuronal–glial tumor (Grades I and II) and a few others [31]. Pilocytic astrocytoma and diffuse astrocytoma are the two commonest PLGGs [50]. In diagnostic situations, there can be overlap in histological features between the groups. Clinically, PLGGs are often regarded as a single group, characterized by good survival and chronicity [3, 35, 54]. Surgical resection is the mainstay of treatment, but adjuvant chemotherapy and radiotherapy are other treatment modalities when tumors are infiltrative or tumors are inaccessible or incompletely resected [2, 60]. However, despite

Rui Ryan Yang, Abudumijiti Aibaidula, and Wei-wei Wang contributed equally.

Electronic supplementary material The online version of this article (<https://doi.org/10.1007/s00401-018-1874-3>) contains supplementary material, which is available to authorized users.

✉ Kay Ka-Wai Li
kayli@cuhk.edu.hk

✉ Ho-Keung Ng
hkng@cuhk.edu.hk

Extended author information available on the last page of the article

a relatively good long-term survival, 30% of PLGGs still experience progression or recurrence [26, 40].

It has long been known that key molecular pathological changes seen in adult low-grade gliomas, like IDH mutation and 1p19q codeletion, are not applicable to PLGGs [52, 62]. In fact, recent studies have shown PLGGs possess their own molecular pathological feature distinct from adults' [35, 54]. In children, pilocytic astrocytoma is characterized by aberrations of the mitogen-activated protein kinase (MAPK) pathway, and BRAF, an intracellular serine/threonine kinase component of the MAPK pathway, is often activated either by gene rearrangement or mutation [31]. The KIAA1549-BRAF fusions are caused by tandem duplication and rearrangement at chromosome 7q34 between BRAF and a gene centromeric to BRAF, KIAA1549 [5, 23, 38, 51]. The fusion genes have been detected in about 70% of pilocytic astrocytoma and 18–67% of all other PLGGs, such as diffuse astrocytoma, pleomorphic xanthoastrocytoma, pilomyxoid astrocytoma, and ganglioglioma [9, 12, 16, 20]. The most common point mutation in PLGGs occurs at codon 600, and results in an amino acid substitution from valine (V) to glutamic acid (E) [43]. BRAF V600E mutation has been described in 6–17% of PLGGs [14, 29, 38]. CDKN2A is a tumor suppressor gene found on chromosome 9p21 that negatively regulates the cell cycle progression [44]. CDKN2A is deleted in about 20% PLGGs [29] and can be also found in adult gliomas [6, 37, 46, 47]. Analysis of patient-matched low- and high-grade gliomas showed 100% BRAF V600E and 80% of CDKN2A alterations could be traced back to their PLGG counterparts, indicating that BRAF V600E and CDKN2A deletion are early events in PLGGs undergoing transformation [33].

Recent genomic studies also identified *v-myb* avian myeloblastosis viral oncogene homolog (MYB) and *v-myb* avian myeloblastosis viral oncogene homolog-like 1 (MYBL1) as novel genetic aberrations in PLGGs [41, 63]. MYB alteration in PLGGs was initially reported by Tatevossian et al. [58] showing the identification of novel MYB amplifications in pediatric diffuse gliomas. In addition to MYB amplification, subsequent studies identified recurrent MYB/MYBL rearrangements and MYB-QKI rearrangements in a small fraction of PLGGs [4, 41, 58]. MYB and MYBL1 abnormalities can be found in about 10% of PLGGs [63]. However, the clinical significance of these new biomarkers for PLGGs has not been examined.

In this study, we investigated the prevalence of TERTp, H3F3A, BRAF V600E mutations, ATRX loss, KIAA1549-BRAF fusion, CDKN2A deletion, and MYB amplification in a large series of PLGGs. TERTp mutation, H3F3A mutation, and ATRX loss are molecular changes usually linked with high-grade tumors, and these alterations in the occasional PLGGs have not previously been studied [27, 32, 61]. We showed that these biomarkers are not only clinically relevant

in PLGGs on their own, but they also enabled us to establish a risk stratification model for PLGGs. Our results highlight the importance of the incorporation of multiple molecular biomarkers in clinical management for PLGGs.

Materials and methods

Patients and tissue samples

Between years 1998 and 2016, a total of 372 cases of PLGGs (WHO Grade I and Grade II) were diagnosed at Prince of Wales Hospital, Hong Kong, the Huashan Hospital, Shanghai, and the First Affiliated Hospital of Zhengzhou University, Zhengzhou. Formalin-fixed and paraffin-embedded tissues (FFPE) of 289 (289/372; 77.7%) PLGGs were recruited when cases were retrievable and included in this study. All patients were aged 18 or below at the time of diagnosis. Histological diagnoses were reviewed by three pathologists (HKN, HC, AKC). The clinicopathological characteristics of the cohort are summarized in Suppl. Table 1 (Online Resource 1).

Data on patient demographics and therapeutic treatment were obtained from paper and electronic medical records at the institutions. Survival data were ascertained from records of follow-up visits in clinics, or by direct contact with patients or close relatives by telephone. This study was approved by The Joint Chinese University of Hong Kong—New Territories East Cluster Clinical Research Ethics Committee, Ethics Committees of Huashan Hospital, Shanghai, and First Affiliated Hospital of Zhengzhou University, Zhengzhou.

Detection of TERTp, H3F3A, BRAF, FGFR1, and IDH1/2 mutations

DNA for mutational analysis was obtained from FFPE tissues according to previous reported procedures [30]. PCR and Sanger sequencing were conducted to examine hotspot mutations at promoter regions (–228 and –250) of TERT, codons 27 and 34 of H3F3A, codon 600 of BRAF, codons 546 and 656 of FGFR1, codon 132 of IDH1, and codon 172 of IDH2 as described previously [1]. PCR was performed in a 10 µl contained 0.5 µl cell lysate, 1 × KAPA2G Robust HotStart ReadyMix (Sigma) or 1 × KAPA HiFi HotStart ReadyMix (Sigma), 0.5 µM of forward and reverse primers. Amplification was conducted under the conditions of 95 °C for 3 min, followed by 45 cycles of 95 °C for 15 s, 60 °C for 15 s, and 72 °C for 30 s on Veriti® 96-well Thermal Cycler (Applied Biosystems). PCR products were cleaned by spin column-based nucleic acid purification kit (iNtRON Biotechnology), and sequenced with BigDye Terminator Cycle Sequencing kit

v1.1 (Life Technologies). The products were resolved in 3130xl Genetic Analysis. Primer sequences are listed in Suppl. Table 2 (Online Resource 2). Representative sequence electropherograms for mutations in TERTp, H3F3A, BRAF, FGFR1, and IDH1 are shown in Suppl. Figure 1 (Online Resource 3).

Fluorescence in situ hybridization (FISH) analysis

KIAA1549-BRAF fusion, MYB amplification, and CDKN2A deletion were evaluated by FISH as described [1, 20]. In KIAA1549-BRAF fusion detection, 3 clones of P1-derived artificial chromosomes spanning the entire BRAF gene (RP4-726N20, RP5-839B19, and RP4-813F11) and a centromeric enumeration probe for chromosome 7 (CEP7) were employed. A commercially available probe was employed for MYB amplification (Cytocell) detection. Vysis LSI CDKN2A SpectrumOrange/CEP 9 SpectrumGreen Probes (Vysis) was employed to investigate CDKN2A deletion. At least 100 non-overlapping signals were counted and analyzed in each case. KIAA1549-BRAF fusion was defined when BRAF:CEP7 ratio was ≥ 1.15 and more than 20% of tumor cells showed relative BRAF gain [19]. MYB amplification was considered when $> 5\%$ of cells displayed clusters or a ratio of target (red) to reference (green) signal > 2 [1]. CDKN2A homozygous deletion was considered when $> 20\%$ of tumor cells showed loss of two signals [20]. Representative photos showing tumors positive for KIAA1549-BRAF fusion, MYB amplification, and CDKN2A deletion are shown in Suppl. Figure 2 (Online Resource 4).

Immunohistochemical detection of ATRX and p53

Expression for ATRX and p53 proteins was determined by immunohistochemistry (IHC) as previously used by this group [30]. Briefly, FFPE tissues of 4 μm thickness were de-waxed in xylene and rehydrated in graded alcohols. Sections were then treated with citrate buffer (pH 6.0) in microwave for antigen retrieval. Immunohistochemical staining was done in BenchMark ULTRA automated tissue staining systems (Ventana Medical Systems, Tucson, AZ, USA). The primary antibodies were anti-ATRX (Sigma HPA001906, 1:400) and anti-p53 (Dako DO-7, 1:100).

For ATRX staining, a tumor was considered ATRX positive when $> 10\%$ of tumor nuclei showed the presence of ATRX expression [59]. Endothelial cells and infiltrating inflammatory cells served as internal positive controls. Cases were classified as failed/non-informative when internal control cells were not immunopositive ($n = 20$ cases). A tumor was scored as p53 positive if $> 10\%$ of tumor nuclei showed strong nuclear staining [56, 57].

RNA extraction

Total RNA was isolated from 5- μm -thick FFPE tissues with RNeasy FFPE kit (Qiagen). RNA quantity and quality was determined using NanoDrop 2000 instrument (ThermoFisher Scientific). Samples with a ratio A260/280 between 1.9 and 2.1 were taken to fusion/duplication detection by NanoString-based platform.

NanoString-based fusion/duplication detection

In an attempt to uncover other genetic alterations in our series of PLGGs that did not exhibit molecular alterations in our list of biomarkers, we employed NanoString nCounter system to detect 33 reported fusion/duplication events in PLGGs. The information of probes for detection of 31 fusion genes and 2 gene duplications in pediatric gliomas was kindly provided by Dr. Cynthia Hawkins at SickKids, Canada [45, 46] [Suppl. Table 3 (Online Resource 5)]. A total of 500 ng RNA was added to the nCounter Elements TagSet in hybridization buffer and incubated at 67 °C for 20 h. Samples were then processed on the nCounter Preparation Station and cartridges were scanned at 555 fields of view on the nCounter Digital Analyzer. Raw NanoString counts were subjected to normalization using counts obtained for positive control probe sets. The normalized data was then subjected to background noise subtraction. A statistical outlier detection method was used to detect the presence of fusion/duplication events. Data were viewed using a box plot. A fusion or duplication transcript was considered when the raw count was above the average of the internal positive control raw counts plus $3 \times \text{IQR}$.

Statistical analysis

Statistical analysis was conducted using IBM SPSS software v20 (IBM Corporation, NY, USA). Chi-squared test (χ^2 -test) was used to examine the correlation between molecular markers and clinical parameters. Progression-free survival (PFS) was defined as time from tumor diagnosis to recurrence or progression. Overall survival (OS) was defined as time from diagnosis to death or last follow-up. Survival curves were performed by Kaplan–Meier method. Univariate and multivariate analyses using Cox's proportional hazards regression model were used to determine molecular biomarkers and clinical features associated with patient survival. All hazard ratios were reported with 95% CIs. $P < 0.05$ (two-sided) was considered statistically significant.

Results

Clinical characteristics of PLGGs

A total of 289 PLGGs diagnosed between years 1988 to 2016 were recruited in this study. The mean and median ages at diagnosis were 11 and 12 years old (range 1–18), respectively. The hemispheres were the most prevalent tumor location, accounting for 42.2% (122/289) of the cohort. The distribution of hemispheric tumors was as follows: frontal ($n=50$), parietal ($n=38$), temporal ($n=28$), and occipital ($n=6$) lobes. Midline origins, including third and fourth ventricles ($n=41$), brain stem ($n=18$), thalamus ($n=16$), spinal cord ($n=12$), sellar region ($n=10$), and pineal region ($n=4$), were found in one hundred and one (34.9%) tumors [53]. The remaining around one-fifth of tumors were found in the cerebellum. Survival data were available in 219 patients (75.8%). The average follow-up period of this study was 5.48 years,

and 51.1% of cases with survival data were followed for > 5 years (112 cases). Suppl. Table 1 (Online Resource 1) summarized the clinicopathological characteristics of the cohort. Suppl. Figure 3 (Online Resource 6) summarized the molecular features of all 289 PLGGs.

Univariate Cox proportional hazards analyses were performed, and grading ($p=0.041$), histological type ($p=0.011$), and extent of resection ($p<0.0001$) were highly associated with PFS (Table 1). Grading ($p=0.011$), histological type ($p=0.0008$), location ($p=0.004$) and extent of resection ($p<0.0001$) were associated with OS (Table 1). Age, gender, chemotherapy, and radiotherapy were not a factor contributing to PFS and OS (Table 1).

TERT promoter mutation is a rare negative prognostic marker in PLGGs

TERTp mutation was identified in a small number (7/278 or 2.5%) of tumors, including three C228T and four C250T. Most of the TERTp-mutant tumors were diffuse astrocytoma

Table 1 Univariate Cox proportional hazards regression models of clinical features

Variables	PFS		OS	
	HR (95% CI)	<i>P</i> value	HR (95% CI)	<i>P</i> value
Age	0.996 (0.936–1.059)	0.893	1.050(0.968–1.139)	0.238
Gender				
Male	1		1	
Female	0.884 (0.481–1.624)	0.691	0.842 (0.385–1.841)	0.667
Grade				
Grade I	1		1	
Grade II	1.904 (1.027–3.530)	0.041	3.059 (1.291–7.247)	0.011
Histological type				
Pilocytic astrocytoma	1	0.011	1	0.0008
Diffuse astrocytoma	2.455 (1.239–4.864)	0.010	4.659 (1.821–11.921)	0.001
Others	0.974 (0.432–2.194)	0.949	1.143 (0.349–3.748)	0.825
Location				
Cerebellum	1	0.078	1	0.004
Midline	2.437 (1.059–5.606)	0.036	8.088 (1.833–35.699)	0.006
Hemisphere	1.446 (0.615–3.398)	0.398	3.055 (0.649–14.371)	0.158
Extent of resection				
Total resection	1		1	
Non-total resection	4.755 (2.291–9.870)	<0.0001	6.908 (2.721–17.534)	<0.0001
Radiotherapy				
Yes	1		1	
No	1.462 (0.723–2.957)	0.290	1.183 (0.515–2.717)	0.692
Chemotherapy				
Yes	1		1	
No	0.929 (0.461–1.872)	0.836	0.764 (0.334–1.747)	0.524
Chemo-radiotherapy				
Yes	1		1	
No	1.090 (0.506–2.348)	0.826	0.919 (0.378–2.236)	0.852

n number of cases with data available

[Suppl. Table 1 (Online Resource 1)]. Four TERTp-mutant tumors were located in midline structure (two third and fourth ventricles, one brainstem, and one thalamus). The other TERTp-mutant tumors were found in hemisphere ($n=2$) and cerebellum ($n=1$). Representative cases were

shown in Suppl. Figure 4 (Online Resource 7). The patients with TERTp mutation were associated with older age ($p=0.03$).

Kaplan–Meier survival analysis revealed TERTp mutation was markedly associated with shorter PFS ($p<0.0001$)

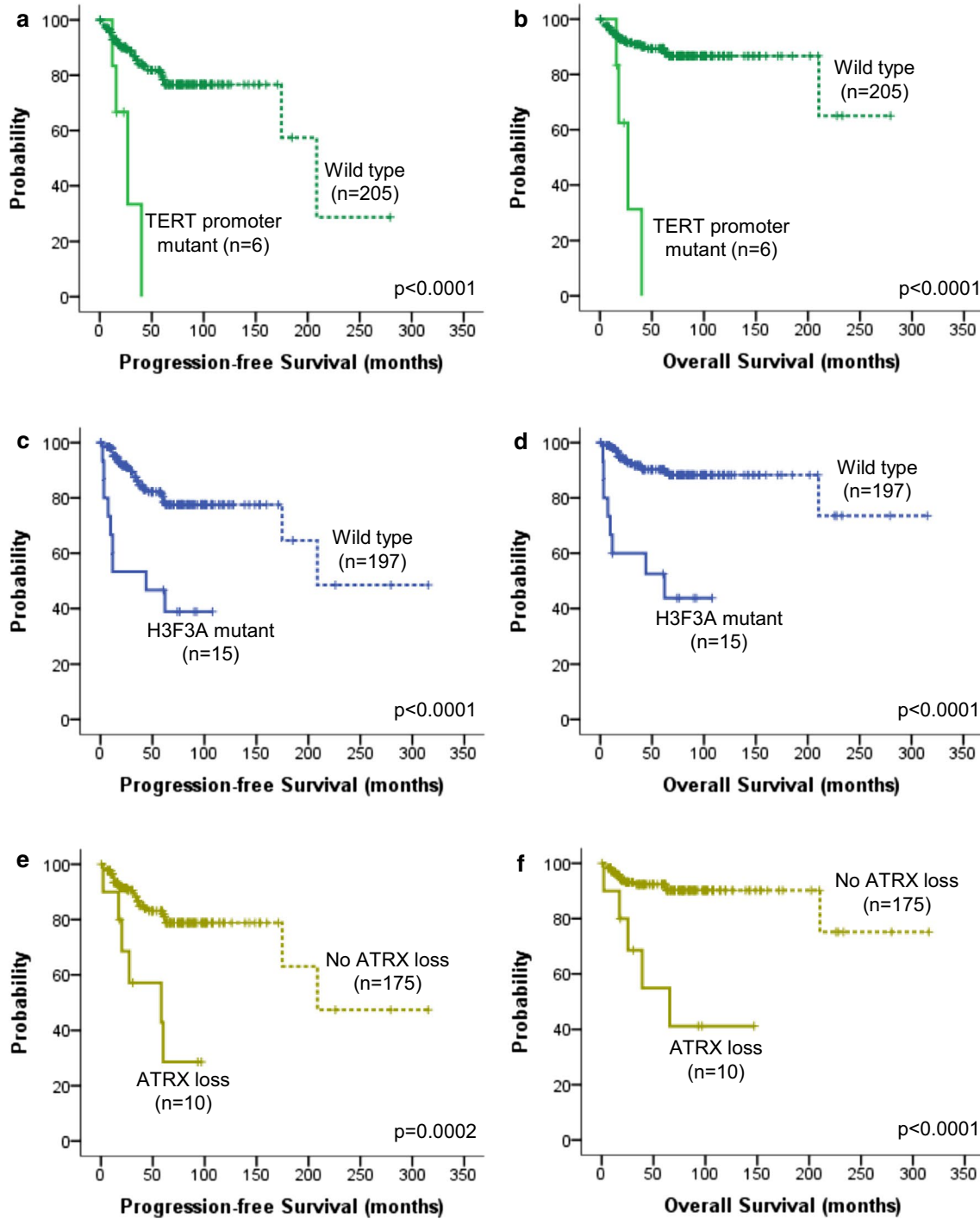


Fig. 1 Kaplan–Meier survival analysis of TERTp, H3F3A, and ATRX. TERTp mutation was strongly associated with a shorter **a** PFS ($p<0.0001$) and **b** OS ($p<0.0001$) in PLGGs. H3F3A muta-

tion was associated with unfavorable **c** PFS ($p<0.0001$) and **d** OS ($p<0.0001$). ATRX loss was associated with poor **e** PFS ($p=0.0002$) and **f** OS ($p<0.0001$)

and OS ($p < 0.0001$) (Fig. 1a, b). After adjustment by age, grade, histology, tumor location, and extent of resection in multivariate analysis, the association of TERTp mutation with PFS and OS did no longer reach statistical significance.

We then examined if these TERTp-mutated-PLGGs harbored 1p19q codeletion, PTEN loss, EGFR amplification, PDGFRA amplification, ATRX loss, and p53 nuclear accumulation, which are common molecular changes found in adult gliomas. We did not detect 1p19q codeletion, PTEN loss, and PDGFRA amplification by FISH analyses in any of these TERTp-mutant tumors (data not shown). By immunohistochemistry, none of these tumors demonstrated ATRX loss or p53 nuclear accumulation. Nevertheless, EGFR amplification was observed in 2/7 (28.6%) of TERTp-mutant tumors. The results suggest PLGGs with TERTp mutation infrequently show the common genetic abnormalities found in adult gliomas.

H3F3A mutation is marker for poor prognosis in PLGGs

H3F3A mutation was detected in a small number (18/280 or 6.4%) of PLGGs, with 13 tumors harbored K27M mutation and 5 tumors harbored G34R mutation. Over half of H3F3A mutations (10/18) were found in diffuse astrocytoma, and accounted for 14.7% (10/68) of this entity [Suppl. Table 1 (Online Resource 1), Suppl. Figure 3 (Online Resource 6)]. Most tumors with H3F3A mutation were located in the midline structure ($n = 9$; three brain stem, three spinal cord, two thalamus, and one pineal region). H3F3A mutation was also found in tumors located in hemisphere ($n = 7$) and cerebellum ($n = 2$). Our finding is in line with previous report showing the presence of H3F3A mutation in pediatric low-grade and high-grade gliomas [11, 21, 55, 61]. Representative cases are shown in Suppl. Figure 5 (Online Resource 8).

Around 60% of K27M mutation (8/13 cases) were found in the tumors in the midline structures, including three in brainstem, three in spinal cord, and two in thalamus. Moreover, 80% of G34R mutation in H3F3A (4/5 cases) were located in tumors from the hemispheres. Although we did not detect a correlation between tumor location and mutation type, our finding is in line with previous reports showing a predilection of G34R to the hemispheres, and K27M to midline locations, respectively, in pediatric high-grade gliomas [8, 55]. H3F3A mutation has no relationship with the age of onset of disease in this series ($p = 0.20$). Mutation of H3F3A was mutually exclusive with TERTp mutation.

Kaplan–Meier survival analysis indicated that H3F3A mutation was significantly associated with adverse PFS ($p < 0.0001$) and OS ($p < 0.0001$) (Fig. 1c, d). We applied multivariate analysis using Cox proportional hazards model with age and variables with $p < 0.05$ in univariate analysis as covariates. H3F3A mutation remained an independent

poor prognosticator for PFS [HR 2.76 (95% CI 1.10–6.94); $p = 0.031$] and OS [HR 3.96 (95% CI 1.36–11.53); $p = 0.012$] after adjustment for age, grade, histology, tumor location, and extent of resection.

ATRX loss is associated with poor PFS and OS

Immunohistochemical detection of ATRX was performed in 267 cases. Nuclear loss was identified in 12/247 (4.9%) PLGGs. The result of 20 cases was not informative. Greater than 50% of the ATRX loss-tumors were diffuse astrocytomas [Suppl. Table 1 (Online Resource 1)]. There was a single tumor (diffuse astrocytoma) with a co-occurrence of H3F3A mutation and ATRX loss [Suppl. Figure 3 (Online Resource 6)]. Representative cases can be found in Suppl. Figure 6 (Online Resource 9).

Survival analysis indicated that ATRX loss was markedly associated with shorter PFS ($p = 0.0002$) and OS ($p < 0.0001$) (Fig. 1e, f). Upon adjustment for age, grade, histology, tumor location, and extent of resection, multivariate analysis revealed that ATRX loss remained as an independent prognosticator for PFS [HR 3.85 (95% CI 1.27–11.65); $p = 0.017$], and OS [HR 3.53 (95% CI 1.02–12.24); $p = 0.047$].

BRAF V600E is associated with poor outcomes in a subset of PLGGs

BRAF V600E mutation was found in 21 of 285 (7.4%) tumors [Suppl. Table 1 (Online Resource 1)]. Interestingly, BRAF V600E was enriched in Grade II tumors ($p = 0.0030$) and were more common in females [$p = 0.022$; Suppl. Table 1 (Online Resource 1)]. Moreover, BRAF V600E was enriched in hemispheric tumors [$p = 0.007$; Suppl. Figure 7 (Online Resource 10)]. Except in two cases, TERTp, H3F3A, and BRAF V600E mutation was mutually exclusive [Suppl. Figure 3 (Online Resource 6)]. None of the BRAF V600E tumors demonstrated ATRX loss. BRAF V600E mutation was mutually exclusive with BRAF fusion or MYB amplification in this series [see below; Suppl. Figure 3 (Online Resource 6)].

After removal of tumors with TERTp mutation or H3F3A mutation or ATRX loss, Kaplan–Meier survival analysis revealed that BRAF V600E was associated with a shorter PFS ($p = 0.011$; Fig. 2a) and OS ($p = 0.032$; Fig. 2b). In multivariate analysis, in which age, grade, histology, tumor location, and extent of resection were included, BRAF V600E was significantly correlated with PFS [HR 4.28 (95% CI 1.32–13.90); $p = 0.016$], suggesting that BRAF V600E had an independent impact on tumor progression. The significance for OS [HR 3.32 (95% CI 0.70–15.82); $p = 0.132$] was not achieved.

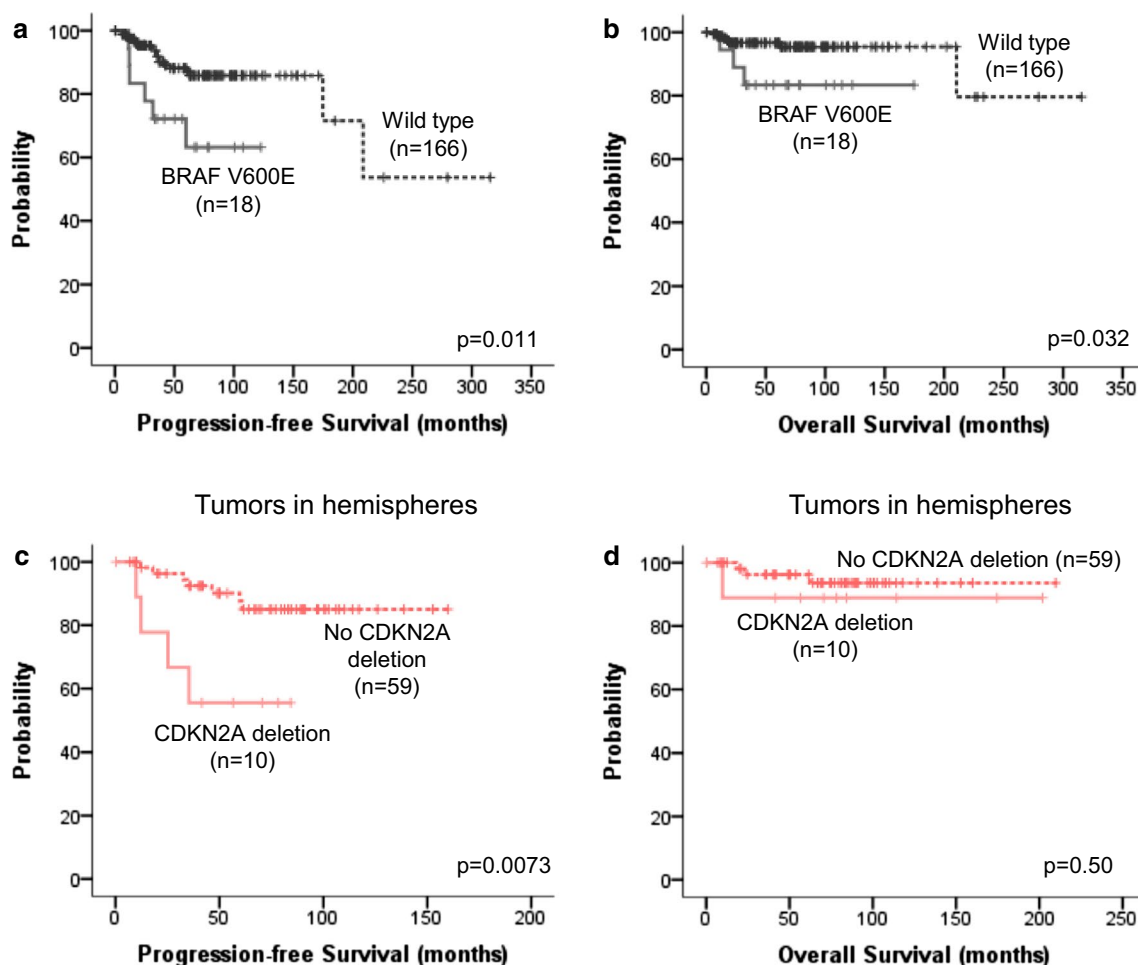


Fig. 2 Kaplan–Meier survival analysis of BRAF V600E and CDKN2A deletion. BRAF V600E was associated with reduced **a** PFS ($p=0.011$) and **b** OS ($p=0.032$). CDKN2A deletion in hemispheric tumors was associated with reduced **c** PFS ($p=0.0073$) but not with **d** OS ($p=0.50$)

Interestingly, BRAF V600E appeared to be more commonly found in infants (0–3 years old). More than 20% (4/19) of infants aged 3 or below displayed BRAF V600E mutation, whereas only 6.4% (17/266) of children (aged > 3–18) bore this mutation [$p=0.041$; Suppl. Table 4 (Online Resource 11)]. BRAF V600E had a significantly negative impact on PFS in the infantile group too [$p=0.0027$; Suppl. Figure 8a (Online Resource 12)] although it did not affect OS ($p=0.081$). Strikingly, in infant, BRAF V600E was more powerful in predicting PFS as compared to histology and grading [Suppl. Figures 8b–c (Online Resource 12)]. We recognize that our infant cohort is small ($n=15$).

CDKN2A deletion in PLGGs

FISH analysis showed CDKN2A deletion in 24/273 (8.8%), a frequency which was consistent with the literature [20, 41, 47]. A strong association between BRAF V600E and CDKN2A deletion was detected [$p=0.0001$; Suppl. Table 5 (Online Resource 13)] [29, 47]. None of the

CDKN2A-deleted tumors carried H3F3A mutation, TERTp mutation, ATRX loss, KIAA1549-BRAF fusion, or MYB amplification [Suppl. Figure 3 (Online Resource 6)].

Over 60% (5/8) of tumors carrying BRAF V600E and CDKN2A were pleomorphic xanthoastrocytoma [Suppl. Figure 3 (Online Resource 6)]. Interestingly, patients with pleomorphic xanthoastrocytoma carrying 2-hits (BRAF V600E and CDKN2A deletion) was markedly younger compared to the rest of pleomorphic xanthoastrocytoma patients without 2-hits ($p<0.0001$; 8.0 ± 1.48 vs 15.5 ± 0.67 years). Given that the number of pleomorphic xanthoastrocytoma in this cohort is small, one must interpret the result carefully.

Upon the removal of samples carrying unfavorable prognostic markers (TERTp, H3F3A, and ATRX), a trend towards shorter PFS ($p=0.086$) and OS ($p=0.059$) was identified in CDKN2A-deleted tumors. Furthermore, survival analysis by tumor location revealed a shorter PFS in CDKN2A-deleted tumors located in hemispheres ($p=0.0073$; Fig. 2c) although OS was not significantly different ($p=0.50$; Fig. 2d). The prognostic value of CDKN2A

deletion specifically to hemisphere tumors has been previously reported [20]. In multivariate analysis after adjusting for age, grading, histology, and resection, CDKN2A deletion remained as an independent prognostic factor for PFS [HR 4.38 (95% CI 1.05–18.23); $p=0.043$]. CDKN2A deletion was not a prognostic marker in tumors of midline or cerebellum.

KIAA1549-BRAF fusion confers a good prognosis

KIAA1549-BRAF fusion gene was identified in 87/272 (32.0%) [Suppl. Table 1 (Online Resource 1); Suppl. Figure 3 (Online Resource 6)]. Majority of the fusion gene was identified in pilocytic astrocytoma, accounting for 55.5% (66/119) of the entity. Our finding is in concordance with the literature showing high prevalence of KIAA1549-BRAF fusion in pilocytic astrocytoma [18]. KIAA1549-BRAF fusion was enriched in Grade I tumors [$p=0.0001$; Suppl. Table 1 (Online Resource 1)]. KIAA1549-BRAF

fusion was also associated with tumor location [$p<0.0001$; Suppl. Table 1 (Online Resource 1)], and almost 60% cerebellar PLGGs carried the fusion gene. BRAF V600E and KIAA1549-BRAF fusion occurred in a mutually exclusive fashion, and none of the KIAA1549-BRAF fusion-positive tumors was positive for TERTp or H3F3A mutation, ATRX loss, and CDKN2A deletion.

As illustrated in Fig. 3a, b, Kaplan–Meier survival curve indicated that KIAA1549-BRAF fusion was strongly associated with a better PFS ($p=0.0017$), and a better OS ($p=0.0029$). KIAA1549-BRAF fusion was not an independent prognostic factor in multivariate analysis.

MYB amplification is a favorable prognosticator in PLGGs

MYB amplification was identified in 28/263 (10.6%) tumors, and was found in all histological entities examined in this study [Suppl. Table 1 (Online Resource 1); Suppl.

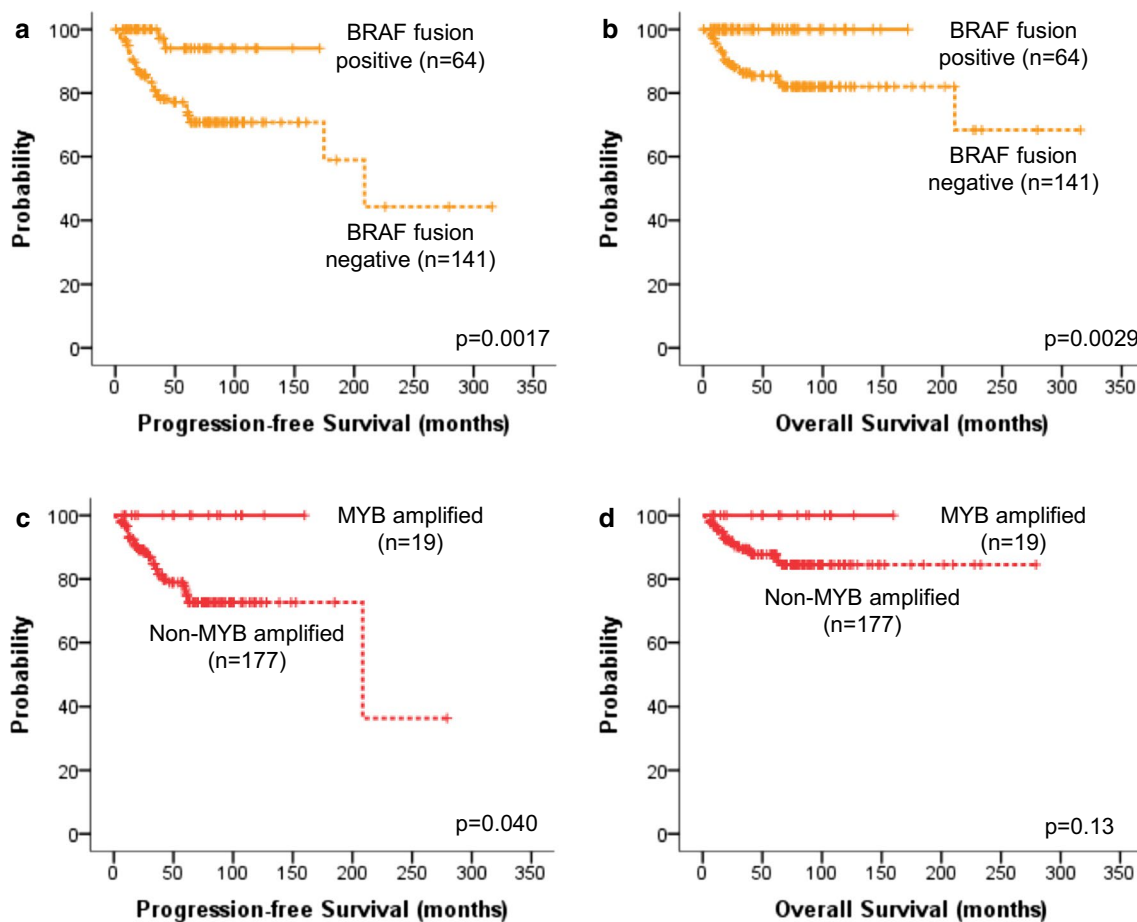


Fig. 3 Kaplan–Meier survival analysis of KIAA1549-BRAF fusion and MYB amplification in PLGGs. Patients with KIAA1549-BRAF fusion had a longer **a** PFS ($p=0.0017$) and **b** OS ($p=0.0029$) compared to patients without KIAA1549-BRAF fusion. Patients with

MYB amplification had a significantly longer **c** PFS ($p=0.040$). No significant difference in **d** OS ($p=0.13$) was observed between patients with and without MYB amplification

Figure 3 (Online Resource 6)]. Other than a case showing both KIAA1549-BRAF fusion and MYB amplification, KIAA1549-BRAF fusion and MYB amplification occurred in a mutually exclusive fashion [Suppl. Figure 3 (Online Resource 6)]. Furthermore, none of MYB-amplified cases carried TERTp, H3F3A, or BRAF V600E mutation, ATRX loss, or CDKN2A deletion.

Survival analysis using Kaplan–Meier survival curves revealed a longer PFS in patients with MYB amplification as compared to patients without MYB amplification ($p=0.040$; Fig. 3c). However, MYB amplification did not independently impact on PFS as shown by multivariate analysis. MYB amplification was also not prognostically relevant in OS ($p=0.13$; Fig. 3d).

FGFR1 mutation and IDH1/2 mutation

Two hotspot mutations in the residues N546 and K656 of the kinase domain of FGFR1 leading to constitutive activation of the growth cascade have previously been identified in the literature in PLGGs [15, 22]. Out of 271 PLGGs with tissue available for mutational analysis, we observed only an oligodendroglial from a 16-year-old girl harbored a mutation at codon K656 of FGFR1 which resulted in a change in amino acid from lysine to glutamic acid. This tumor showed no molecular alteration in TERTp, H3F3A, CDKN2A, BRAF, or MYB.

Mutations of IDH1 or, less frequently, IDH2 have been identified in the majority of adult low-grade gliomas and secondary glioblastoma [62], and it is well established that IDH1/2 mutation is associated with a good clinical outcomes in adult gliomas. In our cohort, IDH1 mutation was found only in 2/260 (0.77%) of cases. Co-occurrence of IDH1 mutation and KIAA1549-BRAF fusion was noted only in one case, an 18-year-old boy with a hemispheric tumor. The other IDH1-mutant tumor showed loss of ATRX expression. No IDH2 mutation was identified. Our data supported previous observations that IDH1/2 mutation is a very rare event in PLGGs [62].

Immunohistochemical detection of p53

We tried to carry out immunohistochemistry to detect p53 expression in 104 tumors that were negative for TERTp, H3F3A, ATRX, BRAF, CDKN2A or MYB, but only 97 cases possessed sufficient tissues for immunostaining. Intense nuclear p53 expression was found in 4/97 (4.1%) of tumors. No significance was detected between p53 immunostaining and age, tumor location, and histology.

NanoString assay analysis

To further explore other genetic alterations in our cohort of PLGGs showing no changes in TERTp, H3F3A, ATRX, BRAF, CDKN2A or MYB, we employed NanoString nCounter system to detect 33 reported fusion/duplication events in PLGGs.

A total of 104 cases were negative for molecular markers examined. Out of these samples, 39/104 (37.5%) samples had sufficient tissue for RNA extraction and were successfully studied. The presence of fusion/duplication events was identified in 6/39 (15.4%) samples. Out of these six tumors, two cases demonstrated FGFR1 duplication [Suppl. Figure 9 (Online Resource 14)]. One pilocytic astrocytomas carried fusion transcript for FGFR1 (exon 17)–TACC1 (exon 7) [Suppl. Figure 9 (Online Resource 14)]. Fusion transcript of ETV6 (exon 1)–NTRK3 (exon 18) was found in 2 diffuse astrocytomas and 1 tumor of other entities. None of the examined cases demonstrated BRAF fusion, confirming our FISH analyses. A prognostic association was not found for any of these genetic abnormalities.

Combined molecular risk stratification of pediatric low-grade gliomas

Next, we evaluated if an integrative analysis of TERTp, H3F3A, ATRX, BRAF V600E, CDKN2A deletion, BRAF fusion, and MYB amplification could improve prognostic stratification. As shown in Fig. 4, we divided the tumors ($n=263$) into four groups: low- ($n=114$), intermediate-I- ($n=35$), intermediate-II- ($n=78$), and high-risk ($n=36$). Patients with BRAF fusion or MYB amplification belonged to low-risk group. Patients with BRAF V600E and/or CDKN2A deletion belonged to intermediate-I-risk group. Patients without alteration in any of these biomarkers belonged to intermediate-II-risk group. And patients with TERTp mutation or H3F3A mutation or ATRX loss belonged to high-risk group. We found these four risk groups were associated with differential clinical features [Suppl. Table 6 (Online Resource 15)].

The high-risk group represented 13.7% (36/263) of PLGGs. Male/female ratio was 2.6:1. All tumors of the high-risk group were aged above 3. The age of high-risk group patients was older compared to those in the intermediate-I- and low-risk groups ($p=0.011$). Notably, patients comprising this risk group were mostly Grade II tumors and of diffuse astrocytoma [Suppl. Table 6 (Online Resource 15), $p<0.0001$]. Furthermore, > 50% of high-risk PLGGs were located in the midline [Suppl. Table 6 (Online Resource 15), $p=0.0003$].

The intermediate-I-risk group comprised 13.3% (35/263) of PLGGs. Similar to the high-risk group, a high proportional of intermediate-I-risk group tumors were of Grade

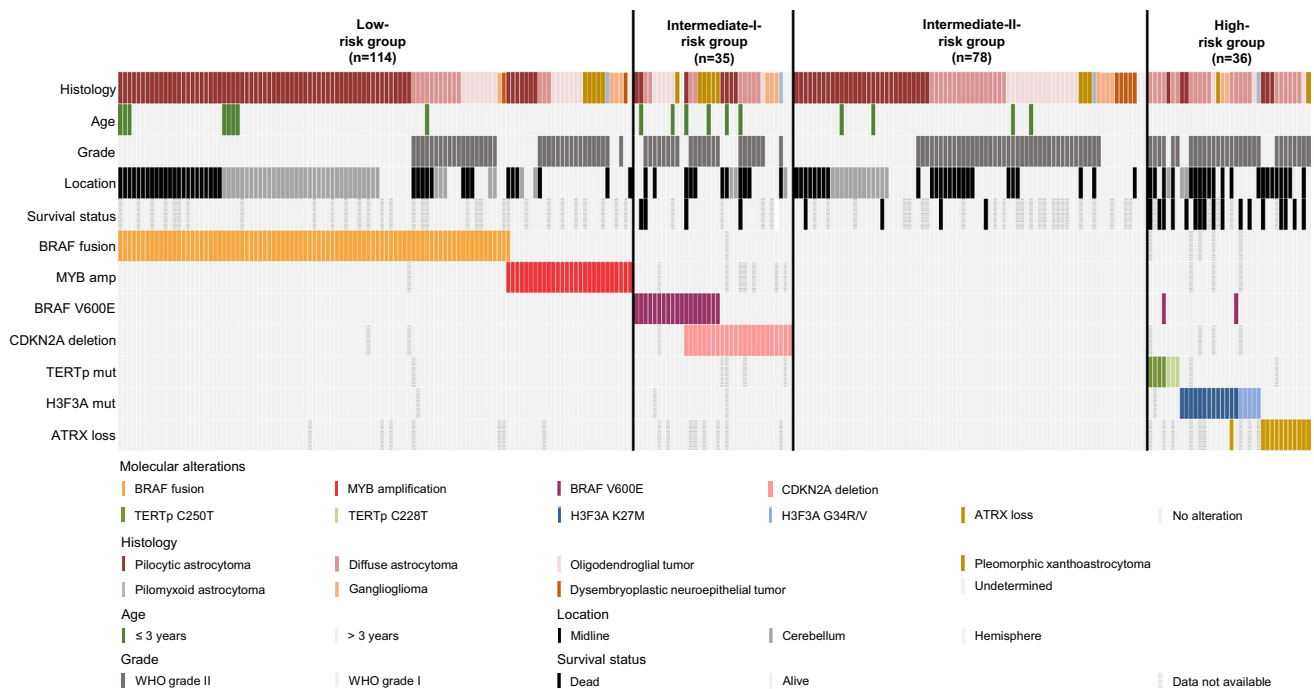


Fig. 4 Summary of clinical data and molecular characteristics of low-, intermediate-I-, intermediate-II-, and high-risk groups. PLGGs were divided into four groups according to molecular markers, TERTp, H3F3A, ATRX, BRAF, CDKN2A, and MYB. The low-risk group ($n = 114$) demonstrated either KIAA1549-BRAF fusion and/or

MYB amplification. The intermediate-I- risk group ($n = 35$) carried BRAF V600E mutation and/or CDKN2A deletion. The intermediate-II- risk group ($n = 78$) did not exhibit alterations in this panel of biomarkers. The high-risk group ($n = 36$) was characterized by the presence of TERTp or H3F3A mutation or ATRX loss

II. Furthermore, majority cases of intermediate-I-risk group were located in the hemispheres [Suppl. Table 6 (Online Resource 15)]. The intermediate-II-risk group accounted for 29.7% (78/263) of PLGGs. In this group, similar frequencies of Grade I (51.3%) and II (48.7%) were found. Around half of the tumors (52.6%) in this risk group were located in the hemispheres.

The low-risk group comprised about 43.3% (114/263) of PLGGs. More than 60% of low-risk group was histologically pilocytic astrocytoma, accounting for 62.6% of this entity. Tumor location was relatively equally distributed in this group [Suppl. Table 6 (Online Resource 15)].

We then compared PFS and OS among risk groups for patients with available clinical data ($n = 198$). We showed these four risk groups exhibited distinct clinical outcomes (Fig. 5a, b, $p < 0.0001$). Of 198 tumors analyzed with univariate Cox regression model, tumor grade, histology, tumor location, extent of resection, and risk group were significantly associated with PFS and OS [Suppl. Table 7 (Online Resource 16)]. In Kaplan–Meier survival analysis, patients of high-risk group exhibited the worst PFS ($p < 0.0001$; Fig. 5a) and OS ($p < 0.0001$; Fig. 5b). Patients of intermediate-I-risk group showed improved PFS and OS compared to those in high-risk group (Fig. 5a, b). Patients of intermediate-II-risk group exhibited similar PFS and OS

compared to those of intermediate-I-risk group, and they in comparison to high-risk patients demonstrated better survival outcomes (Fig. 5a, b). Patients of low-risk group had the most favorable clinical outcomes (Fig. 5a, b). These patients showed excellent survival, and tumor progression was rarely reported. After adjustment of covariates including age, tumor grade, histology, tumor location, and extent of resection in multivariate Cox proportional hazards model, molecular-based risk groups remained independent prognosticators for PFS ($p = 0.0002$; Table 2) and OS ($p = 0.007$; Table 2).

Discussion

Pediatric low-grade gliomas are generally associated with a good long-term survival. While pilocytic astrocytoma is Grade I, even Grade II diffuse gliomas in the pediatric group are associated with a better survival than adults [3, 24, 46]. Yet in spite of the excellent outcome overall, some patients have reduced PFS and OS due to tumor recurrence [3]. Although surgical resection remains the mainstay of treatment, about 30% of pediatric low-grade gliomas are incompletely resected due to the infiltrative nature of tumors or tumors involving critical or inaccessible locations and

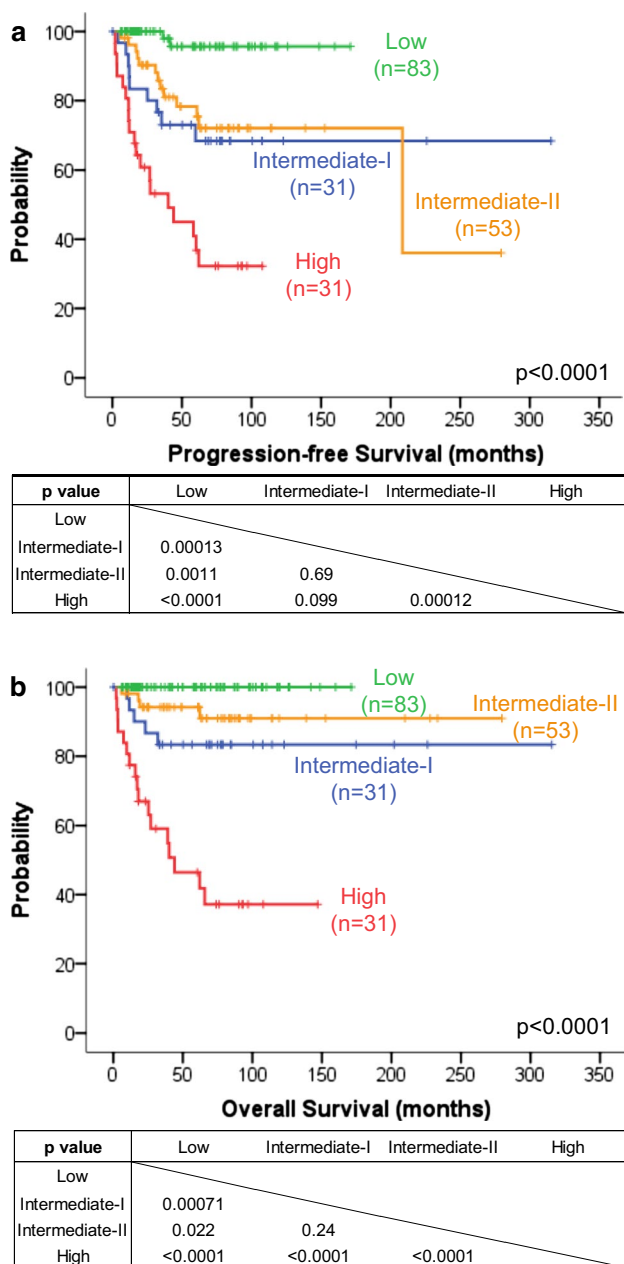


Fig. 5 Risk stratification of PLGGs based on molecular biomarkers. **a** Top and **b** bottom illustrate Kaplan–Meier survival curves of PFS and OS for four risk groups. Green lines indicate survival curves for low-risk group, which had the most favorable PFS and OS. Blue lines represent survival curves for intermediate-I-risk group. Orange lines indicate survival curves for intermediate-II-risk group. Red lines represent survival curves for high-risk group, which showed the worst PFS and OS. The risk groups demonstrated distinct PFS ($p < 0.0001$) and OS ($p < 0.0001$)

they may require adjuvant chemo-radiation [2, 60]. The WHO 2016 classification did not separate adult and pediatric tumors overall, but a large number of WHO tumor entities have association with the pediatric age group [31]. These histological groups have overlapping features and in

small-volume histological samples, are not always clearly distinguishable from one another.

In this study of a large cohort of PLGGs, we are the first group to show that pediatric low-grade gliomas can be separated into low-risk (BRAF fusion or MYB amplification), intermediate-I-risk (BRAF V600E and/or CDKN2A deletion), intermediate-II-risk (no alteration in these biomarkers), and high-risk (TERTp mutation, H3F3A mutation, or ATRX loss) groups with distinct clinical behavior using techniques available in most diagnostic laboratories. We do recognize that the average follow-up is comparatively short (5.48 years) in view of the long survival especially with respect to the low-risk group, and we look forward to seeing similar studies with longer follow-up.

The incidence of ganglioglioma and DNET in our cohort was low compared to the literatures [29, 63]. The former also contributed to an overall lower incidence of BRAF V600E compared to other studies [29, 63]. In our three institutions, we attempted to study FFPE blocks and slides of all retrievable PLGG cases. One possible reason for the fewer ganglioglioma and DNET cases in our cohort is that epileptic surgery for chronic seizure was not part of the service until recently. Our cases were operated on predominantly due to the presence of mass lesions. That might also explain our higher incidence of Grade II tumors and their predominance over the BRAF V600E-positive cases. It is also possible that there is a racial difference in the incidence of these histological types.

TERTp mutation is well known for characterizing both glioblastomas and oligodendrogliomas [27]. It has not previously been reported in pediatric low-grade gliomas. In our cohort, a very small percentage (2.5%) of PLGGs displayed TERTp mutation, and the mutation was associated with a poor prognosis. We further carried out NanoString-based assay to determine if these TERTp-mutated-PLGGs expressed the signature of 33 known fusion/duplication events, such as NTRK, RAF1, and FGFR1/3 fusion genes [Supp. Table 3 (Online Resource 5)]. Four out of the seven tumors had sufficient tissues for the assay. We did not detect fusion/duplication events in any of the four tumors.

H3F3A K27M mutations now characterizing the renamed H3K27M midline glioma with very poor prognosis by the WHO [31], not all of which were midline, have been found in gliomas of various grades [53]. In this large cohort of PLGGs, the number of cases with H3F3A mutations, similar to those with TERTp, is small (6.4%).

Somatic mutations and loss of expression of alpha-thalassemia/mental retardation syndrome X-linked (ATRX) have been detected in 30% of pediatric glioblastomas [49] and 7% of adult glioblastomas [17]. Recently, comprehensive genomic profiling revealed ATRX mutation in a small fraction of PLGGs [21]. The clinical significance of ATRX alteration has not yet elucidated. Our study showed loss of

Table 2 Multivariate Cox proportional hazards regression models of clinical features and risk groups

Variables	PFS		OS	
	HR (95% CI)	<i>P</i> value	HR (95% CI)	<i>P</i> value
Age	0.968 (0.900–1.041)	0.382	1.002 (0.911–1.101)	0.974
Grade				
Grade I	1		1	
Grade II	1.195 (0.234–6.096)	0.830	0.560 (0.052–6.015)	0.632
Histological type				
Pilocytic astrocytoma	1	0.837	1	0.336
Diffuse astrocytoma	1.096 (0.189–6.366)	0.919	2.765 (0.218–35.138)	0.433
Others	0.831 (0.171–4.100)	0.831	1.070 (0.112–10.250)	0.954
Location				
Cerebellum	1	0.899	1	0.320
Midline	1.096 (0.386–3.107)	0.864	2.053 (0.370–11.408)	0.411
Hemisphere	0.911 (0.299–2.776)	0.870	1.024 (0.168–6.250)	0.980
Extent of resection				
Total resection	1		1	
Non-total resection	2.520 (1.095–5.802)	0.030	2.223 (0.729–6.779)	0.160
Risk group				
Intermediate-I-risk group	1	0.0002	1	0.007
High-risk group	3.126 (1.284–7.607)	0.012	3.816 (1.236–11.787)	0.020
Low-risk group	0.132 (0.027–0.656)	0.013	0.000014*	0.907
Intermediate-II-risk group	1.046 (0.420–2.609)	0.923	0.573 (0.145–2.263)	0.427

n number of cases with data available

*The hazard ratio did not have significance

ATRX expression in a low percentage (4.9%) of PLGGs and these tumors behaved poorly. Possession of TERTp mutation or H3F3A mutation or ATRX loss predicts poor prognosis in PLGGs.

BRAF V600E is known to occur in pleomorphic xanthoastrocytoma and ganglioglioma, and also in a small fraction of pilocytic astrocytomas [48, 51]. Compared to Lassaletta et al. study illustrating BRAF V600E mutation in 17.0% of PLGGs, the frequency of BRAF V600E in our cohort is relatively low (7.4%). The difference is likely contributed by the percentage of ganglioglioma in the cohort. In Lassaletta et al. [29] study, 13% of the samples were of ganglioglioma samples and nearly half of them showed BRAF V600E. In contrast, gangliogliomas made up 4.5% of our cohort. We did not feel the bias in ganglioglioma incidence was deliberate. The vast majority of tumors were resected as primarily mass lesions (see cases illustrated), and only until recently, the three hospitals did not carry out brain operations for chronic seizures when small gangliogliomas, DNETs, etc., can be incidental histological findings. There might even be a real ethnic difference in the incidence of ganglioglioma.

BRAF V600E point mutation has been associated with a more aggressive behavior in PLGGs [10, 20, 25, 29, 33]. Lassaletta et al. and Mistry et al. showed that BRAF V600E is a poor prognostic indicator in PLGGs, especially when associated with CDKN2A deletion [29, 33]. Consistent with

previously studies, we also found PLGGs harboring BRAF V600E mutations likely display an increased propensity for progression. Interestingly, the phenomenon seems to occur more commonly among infants (see under “Results”) in our series.

CDKN2A deletion is often found in adult high-grade gliomas and pediatric high-grade gliomas, albeit at lower prevalence [6, 36, 37]. In PLGGs, the incidence of CDKN2A deletion varies from a few percents to around 20% [7, 13, 42, 47], and the frequency in this study does fall within the reported ones. It was found that a subset of pediatric diffuse astrocytomas was characterized by both CDKN2A deletion and BRAF V600E [47]. Moreover, this combination characterized a subset of pediatric low-grade gliomas which transformed to high-grade gliomas [33]. We confirmed a significant association between BRAF V600E and CDKN2A deletion. Presence of BRAF V600E and/or CDKN2A deletion placed tumors into an intermediate-I-risk group.

KIAA1549-BRAF fusion was found in 32.0% of this large cohort. In our cohort, 55.5% of pilocytic astrocytoma demonstrated fusion gene. Horbinski also reported high incidence of KIAA1549-BRAF fusion in pilocytic astrocytoma [19]. Irrespective of the histological designations, 59.1% of our cerebellar tumors demonstrated BRAF fusion [Suppl. Table 1 (Online Resource 1)]. In other studies, cerebellar tumors were shown to carry BRAF fusion at

higher frequency (74.2–89.7%) [19, 21, 63]. There might be a minor racial difference between our series compared to Western series.

There is still debate over the clinical relevance of fusion status. Two studies demonstrated an improved outcome in PLGGs carried KIAA1549-BRAF fusion genes [17, 21]. On the other hand, other reports did not identify the survival benefit of fusion gene [9, 20, 24]. In our study, the presence of KIAA1549-BRAF fusion positive compared to fusion negative was associated with favorable PFS and OS in PLGGs.

MYB alterations including amplifications and rearrangements resulting in elevated MYB protein expression were found in Tatevosian et al.'s [58] series of PLGGs. Whole genome sequencing has also identified 25% of diffuse cerebral gliomas carried abnormalities in MYB and MYBL1 [63]. However, the prognostic values of MYB or MYBL1 alterations have not been explored [28, 39, 63]. In our cohort, MYB amplification was found in ~10% of PLGGs, and was associated with a longer PFS. The presence of MYB amplification or KIAA1549-BRAF fusion puts PLGGs into low-risk group.

Further studies by NanoString-based assay, Sanger sequencing, and immunohistochemistry to detect reported fusion/duplication events, FGFR1/IDH mutation, and p53 protein expression have not contributed to the risk scheme. In this series, 78 cases did not demonstrate molecular changes in our biomarkers. These tumors behaved in an intermediate manner between the high- and low-risk groups, and were placed into intermediate-II-risk group.

Given that the molecular biomarkers examined in this study mostly appeared in mutually exclusion fashion, we here propose a diagnostic algorithm for risk stratification of PLGGs as shown in Suppl. Figure 10 (Online Resource 17). First, a tumor should be examined for BRAF fusion and MYB amplification, which are the most common alterations found in this study. The presence of BRAF fusion or MYB amplification puts it into low-risk group. Examination of BRAF V600E and CDKN2A deletion should be proceeded with if the tumor is negative for the two markers. Either BRAF V600E or CDKN2A deletion places the tumor into intermediate-I-risk group. Finally, TERTp mutation, H3F3A mutation, and ATRX loss are determined to separate the intermediate-II-risk and high-risk groups. Assessment of these molecular biomarkers can be achieved in routine clinical laboratory. This panel should aid the clinical management of patients with pediatric low-grade gliomas.

Acknowledgements This study was supported by the Health and Medical Research Fund, Hong Kong (reference number 02133146); S. K. Yee Medical Foundation, Hong Kong (reference number 2151229); Children Cancer Foundation, Hong Kong; Shenzhen Science Technology and Innovation Commission (reference number JCYJ20170307165432612); and, Shanghai Municipal Commission of

Health and Family Planning, China (reference number 201540145). We are grateful to Dr. Cynthia Hawkins, SickKids, Toronto, Canada, for allowing us to make use her NanoString panel.

References

1. Aibaidula A, Chan AK-Y, Shi Z, Li Y, Zhang R, Yang R et al (2017) Adult IDH wild-type lower-grade gliomas should be further stratified. *Neuro Oncol* 19:1327–1337
2. Ater JL, Zhou T, Holmes E, Mazewski CM, Booth TN, Freyer DR et al (2012) Randomized study of two chemotherapy regimens for treatment of low-grade glioma in young children: a report from the Children's Oncology Group. *J Clin Oncol* 30(21):2641–2647
3. Bandopadhyay P, Berghold G, London WB, Goumnerova LC, Morales La Madrid A, Marcus KJ et al (2014) Long-term outcome of 4,040 children diagnosed with pediatric low-grade gliomas: an analysis of the surveillance epidemiology and end results (SEER) database. *Pediatr Blood Cancer* 61(7):1173–1179
4. Bandopadhyay P, Ramkissoon LA, Jain P, Berghold G, Wala J, Zeid R et al (2016) MYB-QKI rearrangements in angiocentric glioma drive tumorigenicity through a tripartite mechanism. *Nat Genet* 48(3):273–282
5. Bar EE, Lin A, Tihan T, Burger PC, Eberhart CG (2008) Frequent gains at chromosome 7q34 involving BRAF in pilocytic astrocytoma. *J Neuropathol Exp Neurol* 67(9):878–887
6. Bax DA, Mackay A, Little SE, Carvalho D, Viana-Pereira M, Tamber N et al (2010) A distinct spectrum of copy number aberrations in pediatric high-grade gliomas. *Clin Cancer Res* 16(13):3368–3377
7. Broniscer A, Baker SJ, West AN, Fraser MM, Proko E, Kocak M et al (2007) Clinical and molecular characteristics of malignant transformation of low-grade glioma in children. *J Clin Oncol* 25(6):682–689
8. Castel D, Philippe C, Calmon R, Dret LL, Truffaux N, Boddart N et al (2015) Histone H3F3A and HIST1H3B K27 M mutations define two subgroups of diffuse intrinsic pontine gliomas with different prognosis and phenotypes. *Acta Neuropathol* 130(6):815–827
9. Cruz GR, Dias Oliveira I, Moraes L, Del Giudice Paniago M, de Seixas Alves MT, Capellano AM et al (2014) Analysis of KIAA1549–BRAF fusion gene expression and IDH1/IDH2 mutations in low grade pediatric astrocytomas. *J Neurooncol* 117(2):235–242
10. Dahiya S, Haydon DH, Alvarado D, Gurnett CA, Gutmann DH, Leonard JR (2013) BRAFV600E mutation is a negative prognosticator in pediatric ganglioglioma. *Acta Neuropathol* 125(6):901–910
11. Diaz AK, Baker SJ (2014) The genetic signatures of pediatric high-grade glioma: no longer a one-act play. *Semin Radiat Oncol* 24(4):240–247
12. Dimitriadis E, Alexiou GA, Tsotsou P, Simeonidi E, Stefanaki K, Patereli A et al (2013) BRAF alterations in pediatric low grade gliomas and mixed neuronal–glial tumors. *J Neurooncol* 113(3):353–358
13. Dougherty MJ, Santi M, Brose MS, Ma C, Resnick AC, Sievert AJ et al (2010) Activating mutations in BRAF characterize a spectrum of pediatric low-grade gliomas. *Neuro Oncol* 12(7):621–630
14. Eisenhardt AE, Olbrich H, Roring M, Janzarik W, Anh TN, Cin H et al (2011) Functional characterization of a BRAF insertion mutant associated with pilocytic astrocytoma. *Int J Cancer* 129(9):2297–2303
15. Gessi M, Moneim YA, Hammes J, Waha A, Pietsch T (2014) FGFR1 N546 K mutation in a case of papillary glioneuronal tumor (PGNT). *Acta Neuropathol* 127(6):935–936

16. Hawkins C, Walker E, Mohamed N, Zhang C, Jacob K, Shirinian M et al (2011) BRAF-KIAA1549 fusion predicts better clinical outcome in pediatric low-grade astrocytoma. *Clin Cancer Res* 17(14):4790–4798
17. Heaphy CM, de Wilde RF, Jiao Y, Klein AP, Edil BH, Shi C et al (2011) Altered telomeres in tumors with ATRX and DAXX mutations. *Science* 333(6041):425
18. Horbinski C (2013) To BRAF or not to BRAF: is that even a question anymore? *J Neuropathol Exp Neurol* 72(1):2–7
19. Horbinski C, Hamilton RL, Nikiforov Y, Pollack IF (2010) Association of molecular alterations, including BRAF, with biology and outcome in pilocytic astrocytomas. *Acta Neuropathol* 119(5):641–649
20. Horbinski C, Nikiforova MN, Hagenkord JM, Hamilton RL, Pollack IF (2012) Interplay among BRAF, p16, p53, and MIB1 in pediatric low-grade gliomas. *Neuro Oncol* 14(6):777–789
21. Johnson A, Severson E, Gay L, Vergilio JA, Elvin J, Suh J et al (2017) Comprehensive genomic profiling of 282 pediatric low- and high-grade gliomas reveals genomic drivers, tumor mutational burden, and hypermutation signatures. *Oncologist* 22(12):1478–1490
22. Jones DT, Hutter B, Jager N, Korshunov A, Kool M, Warnatz HJ et al (2013) Recurrent somatic alterations of FGFR1 and NTRK2 in pilocytic astrocytoma. *Nat Genet* 45(8):927–932
23. Jones DT, Kocialkowski S, Liu L, Pearson DM, Backlund LM, Ichimura K et al (2008) Tandem duplication producing a novel oncogenic BRAF fusion gene defines the majority of pilocytic astrocytomas. *Cancer Res* 68(21):8673–8677
24. Jones DT, Mulholland SA, Pearson DM, Malley DS, Openshaw SW, Lambert SR et al (2011) Adult grade II diffuse astrocytomas are genetically distinct from and more aggressive than their paediatric counterparts. *Acta Neuropathol* 121(6):753–761
25. Jones DT, Witt O, Pfister SM (2018) BRAF V600E status alone is not sufficient as a prognostic biomarker in pediatric low-grade glioma. *J Clin Oncol* 36(1):96
26. Kilday JP, Katharina U, Bouffet B (2014) Targeted therapy in pediatric low-grade glioma. *Curr Neurol Neurosci Rep* 14(4):441
27. Koelsche C, Sahn F, Capper D, Reuss D, Sturm D, Jones DT et al (2013) Distribution of TERT promoter mutations in pediatric and adult tumors of the nervous system. *Acta Neuropathol* 126(6):907–915
28. Lassaletta A, Zapotocky M, Bouffet E, Hawkins C, Tabori U (2016) An integrative molecular and genomic analysis of pediatric hemispheric low-grade gliomas: an update. *Childs Nerv Syst* 32(10):1789–1797
29. Lassaletta A, Zapotocky M, Mistry M, Ramaswamy V, Honnorat M, Krishnaty R et al (2017) Therapeutic and prognostic implications of BRAF V600E in pediatric low-grade gliomas. *J Clin Oncol* 35(25):2934–2941
30. Li YX, Shi Z, Aibaidula A, Chen H, Tang Q, Li KK et al (2016) Not all 1p/19q non-codeleted oligodendroglial tumors are astrocytic. *Oncotarget* 7(40):64615–64630
31. Louis DN, Perry A, Reifenberger G, von Deimling A, Figarella-Branger D, Cavenee WK et al (2016) The 2016 World Health Organization classification of tumors of the central nervous system: a summary. *Acta Neuropathol* 131(6):803–820
32. Mackay A, Burford A, Carvalho D, Izquierdo E, Fazal-Salom J, Taylor KR et al (2017) Integrated molecular meta-analysis of 1000 pediatric high-grade and diffuse intrinsic Pontine Glioma. *Cancer Cell* 32(4):520–537
33. Mistry M, Zhukova N, Merico D, Rakopoulos P, Krishnaty R, Shago M et al (2015) BRAF mutation and CDKN2A deletion define a clinically distinct subgroup of childhood secondary high-grade glioma. *J Clin Oncol* 33(9):1015–1022
34. Ostrom QT, Gittleman H, Fulop J, Liu M, Blanda R, Kromer C et al (2015) CBTRUS statistical report: primary brain and central nervous system tumors diagnosed in the United States in 2008–2012. *Neuro Oncol* 17(Suppl 4):iv1–iv62
35. Packer RJ, Pfister S, Bouffet E, Avery R, Bandopadhyay P, Bornhorst M et al (2017) Pediatric low-grade gliomas: implications of the biologic era. *Neuro Oncol* 19(6):750–761
36. Paugh BS, Broniscer A, Qu C, Miller CP, Zhang J, Tatevossian RG et al (2011) Genome-wide analyses identify recurrent amplifications of receptor tyrosine kinases and cell-cycle regulatory genes in diffuse intrinsic pontine glioma. *J Clin Oncol* 29(30):3999–4006
37. Paugh BS, Qu C, Jones C, Liu Z, Adamowicz-Brice M, Zhang J et al (2010) Integrated molecular genetic profiling of pediatric high-grade gliomas reveals key differences with the adult disease. *J Clin Oncol* 28(18):3061–3068
38. Pfister S, Janzarik WG, Remke M, Ernst A, Werft W, Becker N et al (2008) BRAF gene duplication constitutes a mechanism of MAPK pathway activation in low-grade astrocytomas. *J Clin Invest* 118(5):1739–1749
39. Qaddoumi I, Orisme W, Wen J, Santiago T, Gupta K, Dalton JD et al (2016) Genetic alterations in uncommon low-grade neuroepithelial tumors: BRAF, FGFR1, and MYB mutations occur at high frequency and align with morphology. *Acta Neuropathol* 131(6):833–845
40. Raabe E, Kieran MW, Cohen KJ (2013) New strategies in pediatric gliomas: molecular advances in pediatric low-grade gliomas as a model. *Clin Cancer Res* 19(17):4553–4558
41. Ramkissoon LA, Horowitz PM, Craiga JM, Ramkissoon SH, Rich BE, Schumacher SE et al (2013) Genomic analysis of diffuse pediatric low-grade gliomas identifies recurrent oncogenic truncating rearrangements in the transcription factor MYBL1. *Proc Natl Acad Sci USA* 110(20):8188–8193
42. Rodriguez EF, Scheithauer BW, Giannini C, Rynearson A, Cen L, Hoesley B et al (2011) PI3 K/AKT pathway alterations are associated with clinically aggressive and histologically anaplastic subsets of pilocytic astrocytoma. *Acta Neuropathol* 121(3):407–420
43. Rodriguez FJ, Lim KS, Bowers D, Eberhart CG (2013) Pathological and molecular advances in pediatric low-grade astrocytoma. *Annu Rev Pathol* 8:361–379
44. Ruas M, Peters G (1998) The p16INK4a/CDKN2A tumor suppressor and its relatives. *Biochim Biophys Acta* 1378(2):F115–F177
45. Ryall S, Krishnaty R, Arnoldo A, Buczkowicz P, Mistry M, Sidaway R et al (2016) Targeted detection of genetic alterations reveal the prognostic impact of H3K27 M and MAPK pathway aberrations in paediatric thalamic glioma. *Acta Neuropathol Commun* 4(1):93
46. Ryall S, Tabori U, Hawkins C (2017) A comprehensive review of paediatric low-grade diffuse glioma: pathology, molecular genetics and treatment. *Brain Tumor Pathol* 34(2):56–61
47. Schiffman JD, Hodgson JG, VandenBerg SR, Flaherty P, Polley MY, Yu M et al (2010) Oncogenic BRAF mutation with CDKN2A inactivation is characteristic of a subset of pediatric malignant astrocytomas. *Cancer Res* 70(2):512–519
48. Schindler G, Capper D, Meyer J, Janzarik W, Omran H, Herold-Mende C et al (2011) Analysis of BRAF V600E mutation in 1320 nervous system tumors reveals high mutation frequencies in pleomorphic xanthoastrocytoma, ganglioglioma and extra-cerebellar pilocytic astrocytoma. *Acta Neuropathol* 121(3):397–405
49. Schwartzentruber J, Korshunov A, Liu XY, Jones DT, Pfaff E, Jacob K et al (2012) Driver mutations in histone H3.3 and chromatin remodelling genes in paediatric glioblastoma. *Nature* 482(7384):226–231
50. Sievert AJ, Fisher MJ (2009) Pediatric low-grade gliomas. *J Child Neurol* 24(11):1397–1408
51. Sievert AJ, Jackson EM, Gai X, Hakonarson H, Judkins AR, Resnick AC et al (2009) Duplication of 7q34 in pediatric low-grade astrocytomas detected by high-density single-nucleotide

- polymorphism-based genotype arrays results in a novel BRAF fusion gene. *Brain Pathol* 19(3):449–458
52. Smith JS, Perry A, Borell TJ, Lee HK, O'fallon J, Hosek SM et al (2000) Alterations of chromosome arms 1p and 19q as predictors of survival in oligodendrogliomas, astrocytomas, and mixed oligoastrocytomas. *J Clin Oncol* 18(3):636–656
 53. Solomon DA, Wood MD, Tihan T, Bollen AW, Gupta N, Phillips JJ et al (2016) Diffuse midline gliomas with histone H3-K27M mutation: a series of 47 cases assessing the spectrum of morphologic variation and associated genetic alterations. *Brain Pathol* 26(5):569–580
 54. Sturm D, Pfister SM, Jones DTW (2017) Pediatric gliomas: current concepts on diagnosis, biology, and clinical management. *J Clin Oncol* 35(21):2370–2377
 55. Sturm D, Witt H, Hovestadt V, Khuong-Quang DA, Jones DTW, Konermann C et al (2012) Hotspot mutations in H3F3A and IDH1 define distinct epigenetic and biological subgroups of glioblastoma. *Cancer Cell* 22(4):425–437
 56. Takami H, Yoshida A, Fukushima S, Arita H, Matsushita Y, Nakamura T et al (2015) Revisiting TP53 mutations and immunohistochemistry—a comparative study in 157 diffuse gliomas. *Brain Pathol* 25(3):256–265
 57. Tanboon J, Williams EA, Louis DN (2016) The diagnostic use of immunohistochemical surrogates for signature molecular genetic alterations in gliomas. *J Neuropathol Exp Neurol* 75(1):4–18
 58. Tatevossian RG, Tang B, Dalton J, Forshew T, Lawson AR, Ma J et al (2010) MYB upregulation and genetic aberrations in a subset of pediatric low-grade gliomas. *Acta Neuropathol* 120(6):731–743
 59. Wiestler B, Capper D, Holland-Letz T, Korshunov A, von Deimling A, Pfister SM et al (2013) ATRX loss refines the classification of anaplastic gliomas and identifies a subgroup of IDH mutant astrocytic tumors with better prognosis. *Acta Neuropathol* 126(3):443–451
 60. Wisoff JH, Sanford RA, Heier LA, Sposto R, Burger PC, Yates AJ et al (2011) Primary neurosurgery for pediatric low-grade gliomas: a prospective multi-institutional study from the Children's Oncology Group. *Neurosurgery* 68(6):1548–1554 (**discussion 1554–1545**)
 61. Wu G, Broniscer A, McEachron TA, Lu C, Paugh BS, Beckskfort J et al (2012) Somatic histone H3 alterations in pediatric diffuse intrinsic pontine gliomas and non-brainstem glioblastomas. *Nat Genet* 44(3):251–253
 62. Yan H, Parsons DW, Jin G, McLendon R, Rasheed BA, Yuan W et al (2009) IDH1 and IDH2 mutations in gliomas. *N Engl J Med* 360(8):765–773
 63. Zhang J, Wu G, Miller CP, Tatevossian RG, Dalton JD, Tang B et al (2013) Whole-genome sequencing identifies genetic alterations in pediatric low-grade gliomas. *Nat Genet* 45(6):602–612

Affiliations

Rui Ryan Yang^{1,2,3} · Abudumijiti Aibaidula³ · Wei-wei Wang⁴ · Aden Ka-Yin Chan¹ · Zhi-feng Shi³ · Zhen-yu Zhang⁵ · Danny Tat Ming Chan⁶ · Wai Sang Poon⁶ · Xian-zhi Liu⁵ · Wen-cai Li⁴ · Rui-qi Zhang¹ · Yan-Xi Li¹ · Nellie Yuk-Fei Chung^{1,2} · Hong Chen⁷ · Jingsong Wu³ · Liangfu Zhou³ · Kay Ka-Wai Li^{1,2} · Ho-Keung Ng^{1,2}

¹ Department of Anatomical and Cellular Pathology, The Chinese University of Hong Kong, Prince of Wales Hospital, 30-32 Ngan Shing Street, Shatin, Hong Kong SAR, China

² Shenzhen Research Institute, The Chinese University of Hong Kong, No. 10, 2nd Yuexing Road, Nanshan District, Shenzhen 518057, China

³ Department of Neurosurgery, Huashan Hospital, Fudan University, Wulumuqi Zhong Road 12, Shanghai 200040, China

⁴ Department of Pathology, The First Affiliated Hospital of Zhengzhou University, Jian She Dong Road 1, Zhengzhou 450001, Henan, China

⁵ Department of Neurosurgery, The First Affiliated Hospital of Zhengzhou University, Jianshe Dong Road 1, Zhengzhou 450001, Henan, China

⁶ Department of Neurosurgery, The Chinese University of Hong Kong, Prince of Wales Hospital, 30-32 Ngan Shing Street, Shatin, Hong Kong SAR, China

⁷ Department of Pathology, Huashan Hospital, Fudan University, Wulumuqi Zhong Road 12, Shanghai 200040, China